

# Guide for Processing of Textured Piezoelectric Ceramics Through the Template Grain Growth Method

Temesgen Tadeyos Zate<sup>1</sup>, Jeong-Woo Sun<sup>1</sup>, Nu-Ri Ko<sup>1</sup>, Hye-Lim Yu<sup>1</sup>,  
Woo-Jin Choi<sup>1</sup>, Jae-Ho Jeon<sup>2</sup>, and Wook Jo<sup>1</sup> 

<sup>1</sup> Department of Materials Science and Engineering, Ulsan National Institute of Science and Technology (UNIST), Ulsan 44919, Korea

<sup>2</sup> Department of Functional Powder Materials, Korea Institute of Materials Science, Changwon 51508, Korea

(Received May 15, 2023; Revised May 22, 2023; Accepted May 24, 2023)

**초록:** 압전 세라믹스는 전기에너지와 기계에너지를 상호 전환할 수 있는 성질을 기반으로 액추에이터 및 트랜스듀서 등에 사용되는 핵심 소재이다. 결정배향 성장법(TGG)은 다결정 세라믹스의 압전 특성을 획기적으로 향상시킬 수 있는 방법으로 많은 주목을 받고 있다. 하지만, TGG 방식을 통해 결정립을 배향하는 과정은 여러 단계의 최적화가 필요하기 때문에 입문자에게는 상당히 도전적인 기술이다. 따라서 이 기고문에서는 입문자의 입장에서 TGG를 가장 쉽게 접근할 수 있도록 납작한 모양의 템플릿을 합성하기 위한 용융염 합성기법 및 실제 결정배향을 위한 Tape Casting 과정 나아가 배향도를 향상시키기 위해 주의할 점에 이르기까지 TGG 전반에 대한 내용을 제공하고자 한다. 본 기고문이 TGG 방법에 대한 이해도를 높이고 활용 및 개선하고자 하는 모든 연구자들에게 정보 및 통찰을 제공할 수 있는 기본 참고서가 되기를 희망한다.

**키워드:** 압전 세라믹, 결정배향 성장법, 용융염 합성, 테이프캐스팅

**Abstract:** The templated grain growth (TGG) method has gained significant attention for its ability to produce highly textured piezoelectric ceramics with significantly enhanced performance, making it a promising method for transducer and actuator applications. However, the texturing process using the TGG method requires the optimization of multiple steps, which can be challenging for beginners in this field. Therefore, in this tutorial, we provide an overview of the TGG method mainly based on our previous published works, including its various processing steps such as synthesizing anisotropic-shaped templates with size and size distribution control using the molten salt synthesis technique, tape casting, and identifying key factors for proper alignment of the templates in the target matrix system. Our goal is to provide a resource that can serve as a basic reference for researchers and engineers looking to improve their understanding and utilization of the TGG method for producing textured piezoelectric ceramics.

**Keywords:** Templated grain growth, Molten salt synthesis, Anisotropic-shaped templates, Tape casting

---

✉ Wook Jo; [wookjo@unist.ac.kr](mailto:wookjo@unist.ac.kr)

## 1. INTRODUCTION

Copyright ©2023 KIEEME. All rights reserved.

This is an Open-Access article distributed under the terms of the Creative Commons Attribution Non-Commercial License (<http://creativecommons.org/licenses/by-nc/3.0>) which permits unrestricted non-commercial use, distribution, and reproduction in any medium, provided the original work is properly cited.

- Piezoelectric ceramics convert electrical energy to mechanical energy and vice versa, and therefore they have a wide range

of applications in various areas such as sensors, actuators, energy harvesting, and biomedical devices. Their performance is highly dependent on the crystallographic orientation of the grains in the material [1].

- Texturing of piezoelectric ceramics, specific along (001) crystallographic direction can significantly enhance the performance. The templated grain growth (TGG) method is a promising approach for producing textured ceramics with controlled grain orientation. In this method, anisotropic-shaped templates are used to assist the orientation of the ceramic grains during the growth process [1].
- Typically, the process of texturing involves several steps, which include preparing plate-like templates, aligning them within matrix powders using tape casting or screen-printing techniques, and allowing the templates to grow during sintering.
- The classification of texturing methods into three groups - TGG, RTGG (reactive TGG), and HTGG (hetero TGG) - as depicted in Figs. 1(a), (b), and (c), depends on factors such as the chemical composition and crystal structure of both the template and matrix, as well as the chemical reaction between them [1,2].
- The TGG method, depicted in Fig. 1(a), involves using a template and matrix made from the same chemical composition and crystal structure, as explained in reference [3]. This method preserves the properties of the material, but the availability of template particles is limited.
- The RTGG method, depicted in Fig. 1(b), involves using reactive template particles and complementary compound particles having a different chemical composition, as well

as a reaction that occurs during the calcination process causing the template and the matrix to become the same in chemical composition. The template then grows during the sintering process, like the TGG method. This method has the advantage of producing final textured ceramics of the same chemical composition, but obtaining reactive template particles can be challenging. Furthermore, as explained in reference [4], the RTGG method is similar to the TGG method except that it is a combination of a chemical reaction between the template and complementary compound particles that occurs during calcination resulting in the initial state of TGG.

- The HTGG method, depicted in Fig. 1(c), involves using hetero-templates and matrix particles with different chemistry, where the template grows during sintering by consuming fine matrix particles, while the initial hetero-templates remain in the core of grown textured grain. This method is used when suitable templates of the same chemical composition or reactive templates are unavailable. In addition, the templates must be chemically stable and not react with the matrix to form a liquid or a second phase during sintering [5].
- To achieve a high degree of texture using the TGG method, several factors such as the size and shape of the templates, the stability of the template in the matrix system, the tape casting process, and the alignment of the templates in the target matrix system need to be carefully processed [6,7]. Among several factors, good texture also depends on the amount of template volume fraction and sintering temperature [6,7]. In light of this, the objective of this tutorial is to

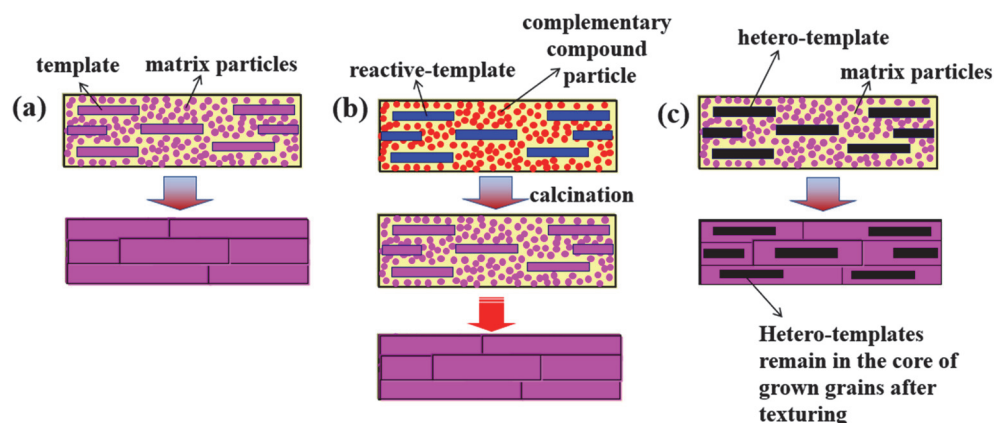


**Fig. 1.** Illustration of three different template-based methods for producing textured ceramics - (a) TGG, (b) RTGG, and (c) HTGG.

provide a comprehensive overview of the TGG method, typically HTGG method, and its various processing steps. The tutorial will encompass the synthesis of anisotropic-shaped templates with size and size distribution control utilizing the molten salt synthesis technique, a detailed tape casting process, and the crucial factors that determine the optimal alignment of the templates in the target matrix system. Through these resources, researchers and engineers can enhance their understanding on the utilization of the TGG method for producing textured piezoelectric ceramics.

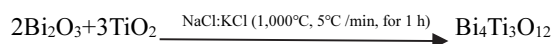
## 2. SYNTHESIS OF AN ANISOTROPIC-SHAPED TEMPLATE

- Anisotropic-shaped templates used in the TGG method need to have a high aspect ratio, generally, greater than 10, and a needle-like or plate-like morphology for optimal alignment during the tape-casting process. Additionally, the lattice constant difference between the template and the matrix is preferred if less than 15% to ensure a good epitaxial match [1,2].
- Several techniques have been used to synthesize anisotropic-shaped templates, including molten-salt synthesis (MSS), flux method, and solid-state reaction (SSR) [8]. Among them, MSS is a highly controlled technique that offers several advantages, including high purity, homogeneity, and control over crystal growth [8].

### 2.1 Synthesis of BaTiO<sub>3</sub> (BT) plate-like template

- The BT template has been widely used for texturing of several Pb-based material systems. Here, the synthesis of a BT plate-like template by MSS is discussed [6,7].

**Step 1:** - Plate-like Bi<sub>4</sub>Ti<sub>3</sub>O<sub>12</sub> (BiT) precursor synthesis



- The process involved the use of a mixture of NaCl and KCl salts in a 1:1 molar ratio mixed using ball milling for 24 h with a stoichiometric mixture of Bi<sub>2</sub>O<sub>3</sub> and TiO<sub>2</sub> (2:3 molar ratio) in a 1:1 ratio with the salt. After drying the mixture

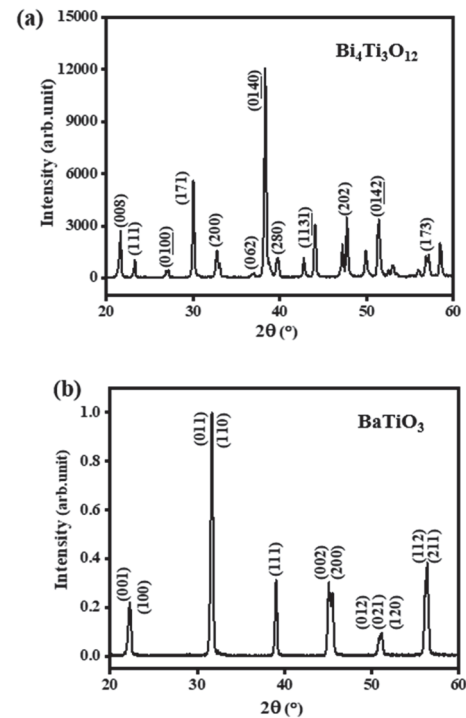
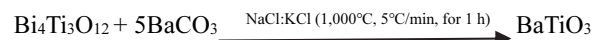


**Fig. 2.** (a) XRD of Bi<sub>4</sub>Ti<sub>3</sub>O<sub>12</sub> and (b) BaTiO<sub>3</sub>.

at 80°C, the mixture undergoes heat treatment at 1,000°C, 5°C/min, for 1 h in a box furnace using a covered alumina crucible. After heat treatment, the result is washed five times with warm DI water (heated on the heating plate at 80°C), to remove Cl ions from the BiT platelets. Finally, the washed powder (BiT) needs drying in the oven at 80°C for 24 h.

**Step 2:** - Plate-like BaTiO<sub>3</sub> (BT) template synthesis



- Next, the BiT precursor combined with BaCO<sub>3</sub> in a 1:5 molar ratio to synthesize the plate-like BT crystals via the topochemical microcrystal conversion (TMC) method as shown in Fig. 1. To prevent damage to the BiT precursor, rather than ball milling, the BiT and BaCO<sub>3</sub> mixture are magnetically stirred at 150 RPM with an equal weight of NaCl and KCl salts in a 1:1 molar ratio for 2 hours in ethanol medium. To obtain plate-like BT crystals, the mixture undergoes drying at 80°C and heated at 1,000°C, 5°C/min, for 1 h in a box furnace using a covered alumina

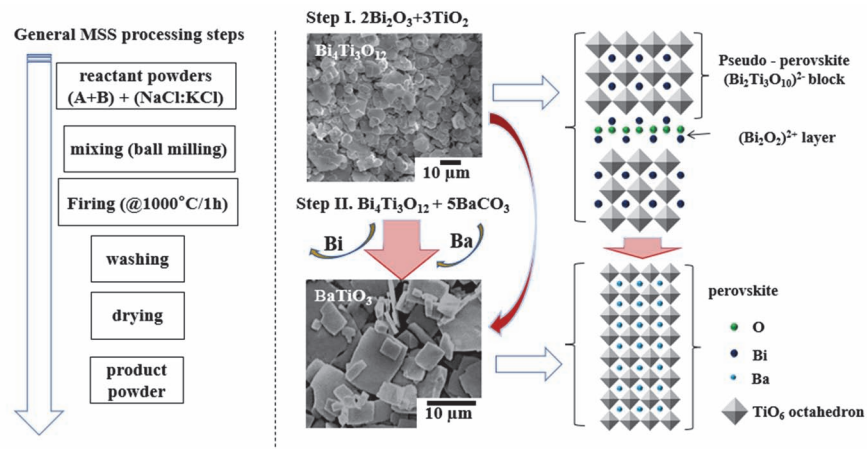


**Fig. 3.** Topochemical microcrystal conversion (two-step synthesis of BT template).

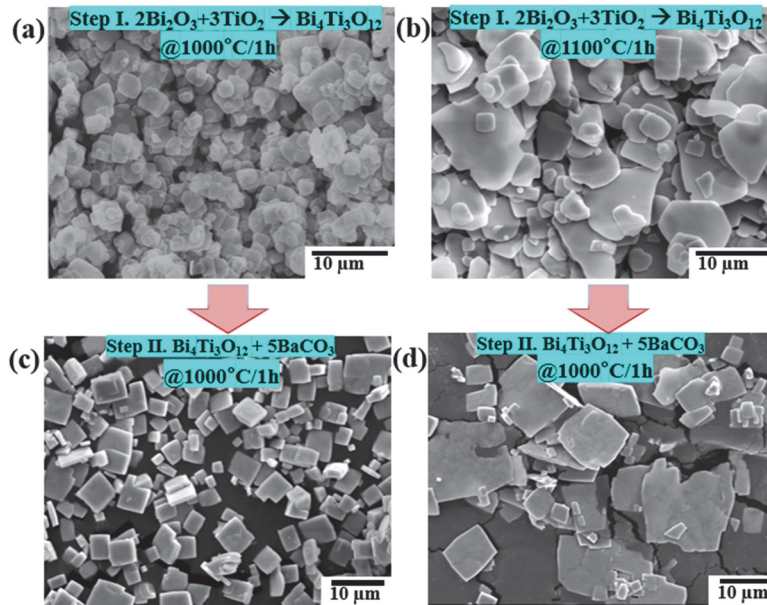


**Fig. 4.** (a) SEM image of BiT template synthesized at 1,000°C for 1 h, (b) SEM image of BiT template synthesized at 1,100°C for 1 h, (c) SEM image of BT template synthesized using the BiT template shown in (a), and (d) SEM image of BT template synthesized using the BiT template shown in (b).

crucible. Finally, to remove the salt and  $\text{Bi}_2\text{O}_3$  by-products, the product needs first melting using 27% concentrated nitric acid by magnetic stirring at 150 RPM, and then washed 3 times with nitric acid and warm DI water, each time acid followed by DI water washing and filtering, which avoids the template not to be etched by the acid.

- After drying the washed powder at 80°C for 24 h, the phase formation, and the microstructure needs to be confirmed using X-ray diffraction (XRD) and Scanning Electron Microscope (SEM) analysis as shown in Figs. 2 and 3.

## 2.2 Controlling the size and size distribution of the template

- The size and shape of the BT template are determined by the size and shape of the BiT precursor, which is possible by adjusting the synthesis temperature or time. Therefore, controlling the morphology of the BiT precursor template can directly influence the morphology of the BT template. For example, Fig. 4(a) and (b) demonstrate that increasing the synthesis temperature of the BiT template from 1,000°C

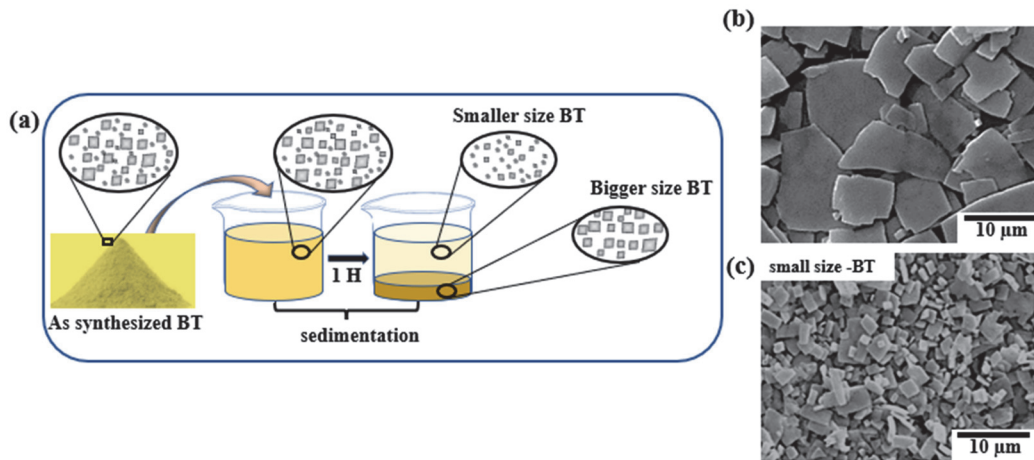


**Fig. 5.** (a) Schematic illustration of the sedimentation process to remove small-sized BT particles, (b) SEM image of the BT template after sedimentation, showing a reduction in the population of smaller templates compared to the as-synthesized BT template shown in Fig. 3(d), and (c) SEM image of removed BT particles (The solvent used for the sedimentation process was deionized water).

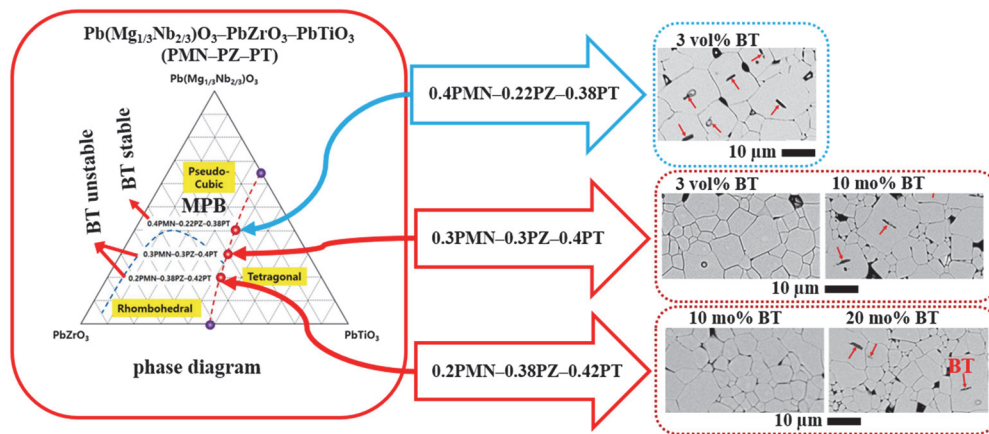


**Fig. 6.** BaTiO<sub>3</sub> template stability in the PMN–PZ–PT material system.

for 1 h to 1,100°C for 1 h led to an increase in the size of the BiT template, increasing the size of the BT template as shown in Fig. 4(c) and (d). Therefore, the synthesis temperature can be adjusted to control the size of the BT template.

- As the as-synthesized BT template in Fig. 4(d) contains small-sized template particles, the size distribution appears to be wide, which leads to the difficulty of optimizing the tape casting blade gap. To obtain a narrow size distribution, the small-sized BT particles (<5 μm) can be removed by the sedimentation process, as shown schematically in Fig. 5(a) and (b) shows the SEM image after revolving small-size BT particles which are shown in Fig. 5(c), where the

smaller templates are less populated compared to the as-synthesized BT template shown in Fig. 4(d) [7].

### 2.3 Hetero-template stability in the matrix system

- Inspecting the stability of the hetero-template, for HTGG, in the target matrix system is necessary as explained in the introduction section. This can be done by mixing a small volume fraction of the template and the matrix by magnetic stirring, drying, pelleting, and then sintering. Then, confirm the stability of the template in the target material, for example, checking the electron backscattered diffraction (EBSD) image of the sintered sample as shown in Fig. 6 [6].

### 3. ALIGNMENT OF THE TEMPLATES IN THE MATRIX SYSTEM

There are several techniques available for aligning the templates, including screen printing and tape casting. Since the processes are pretty much similar, we focus on the tape casting process which allows the fabrication of large scale compared to screen printing as shown in Fig. 7(a) and (b).

#### 3.1 Factors affecting the alignment of the template during tape casting

Figure 8 illustrates the key factors that influence the alignment of templates during the tape-casting process.

These factors include: -

- *The aspect ratio of the template:* - plays a significant role in determining the degree of alignment achieved, with higher aspect ratios, usually 1/10, leading to better alignment.
- *Template to matrix size difference:* - A size difference between the template and the matrix can also affect the alignment, the size of the template is usually effective when 10 times larger than the matrix powder size.
- *Tape casting blade gap and casting speed:* - Generally, a 100  $\mu\text{m}$  to 250  $\mu\text{m}$  blade gap is used for the alignment of the template size ranging between 5  $\mu\text{m}$  to 20  $\mu\text{m}$  [6,7]. For example, as shown in Fig. 9(a), for texturing of PMN–PZ–PT containing 3 vol% of BT, first the blade gap varied from 100  $\mu\text{m}$  to 250  $\mu\text{m}$  while keeping the casting speed at 22

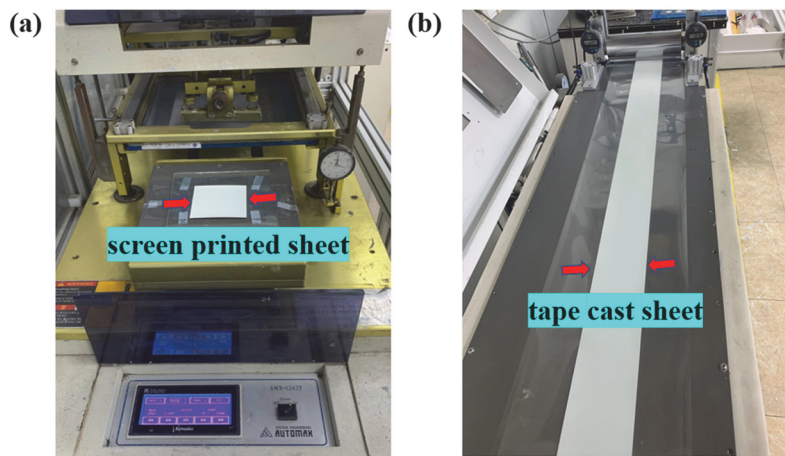


Fig. 7. (a) Screen printing and (b) tape casting (tape casting allows for the fabrication of larger scales compared to screen printing).

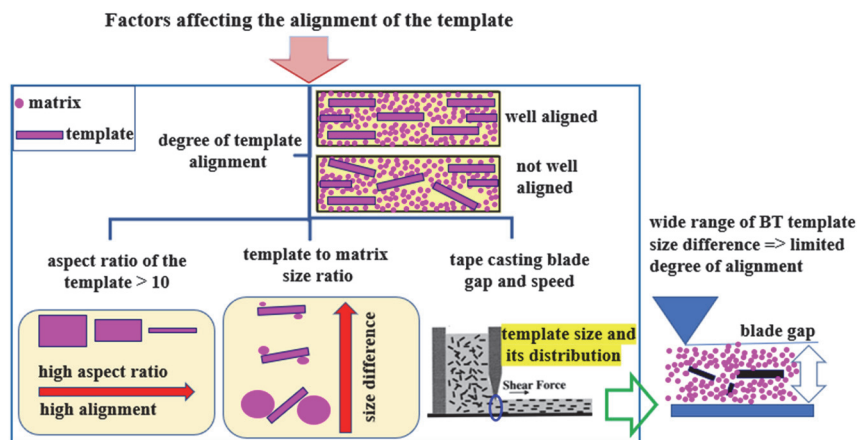
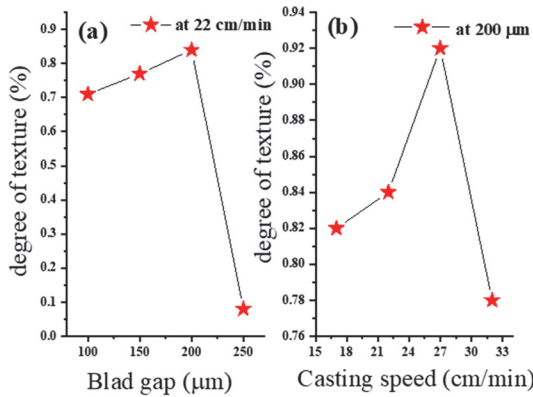


Fig. 8. Illustrates the schematic diagrams of factors affecting the alignment of templates during the tape casting process.



**Fig. 9.** (a) Variation of blade gap while keeping casting speed at 22 cm/min and (b) variation of casting speed while keeping blade gap at 200 μm.

cm/min. The optimum blade gap with respect to the higher degree of texture, which is 200 μm, is then kept constant and the casting speed was varied from 17 cm/min to 33 cm/min resulting in the peak of the degree of texture at 27 cm/min as shown in Fig. 9(b).

## 4. TAPE CASTING

### 4.1 Slurry preparation

In this section, we will illustrate an example of the process of slurry preparation for tape casting, as depicted in Table 1, outlining the optimal conditions that generate a viscosity of about 10,000 cP using spindle number 5 at 30 RPM [6,7].

**Table 1.** Optimal conditions for slurry preparation for tape casting, including the weight percentage of PMN–PZ–PT powder, solvent, dispersant, binder, and plasticizer.

	Matrix	Solvent	Units
Ratio	60	40	[wt%]
Solvent			
	Ethanol	Methyl-ethyl-ketone (MEK)	
Ratio	60	40	[vol]
Dispersant (ceraperse III)			
Ratio	1.67		[wt%]
Binder (polyvinyl butyral (PVB))			
Ratio	10		[wt%]
Plasticizer (di-n-butyl phthalate (DBP))			
Ratio	1.67		[wt%]

Detailed information on the control of viscosity can be found in [9] and the general processing step is shown in Fig. 10(a).

- The slurry was produced by blending 60 wt% PMN–PZ–PT powder with 40 wt% solvents (composed of 60 vol% ethanol and 40 vol% methyl-ethyl-ketone) and 1.67 wt% dispersants (ceraperse III) via ball milling at 200 RPM for a duration of 24 h.
- Following this step, 10 wt% binders (polyvinyl butyral) were added to the mixture and ball milled for an additional 24 h.
- Finally, the appropriate quantity of BT template and 1.67 wt% plasticizers (di-n-butyl phthalate) were included, and the mixture was mixed for an additional 20 min at the same

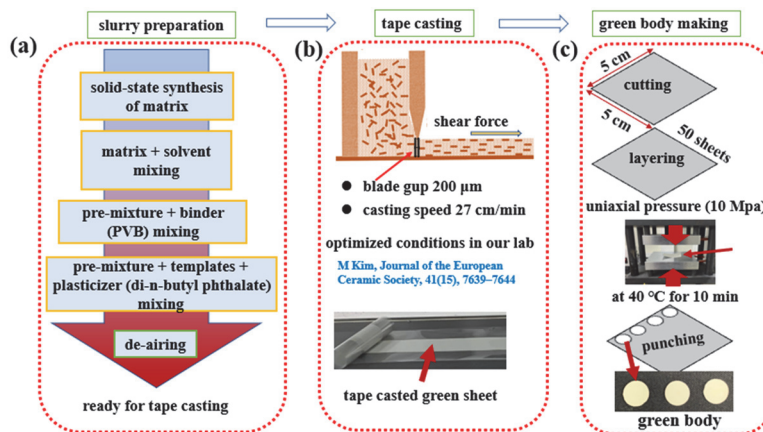


**Fig. 10.** Illustration of the process steps for (a) slurry preparation, (b) tape casting, and (c) green body making.

milling condition but 50 RPM. Before tape casting, mechanical pumping at 10,000 Pa in 5 to 10 min was performed to remove any air from the slurry.

## 4.2 Green body making

- According to Fig. 10(b), the slurry prepared as described above was utilized for tape casting at the blade gap of 200  $\mu\text{m}$  and casting speed of 27 cm/min. Following the tape casting, the sheet was cut into dimensions of 5 cm by 5 cm and 50 layers were subsequently laminated under a uniaxial pressure of 10 Mpa at 40°C for 10 min. The green body can be obtained through the use of a circular punching tool with a diameter of 10 cm to punch the laminated sheet as shown in Fig. 9(c).

## 4.3 Binder burnout

- Figure 11 shows the burnout schedule for the sample prepared in the previous section. The optimization of binder burnout temperature over time requires consideration of the thermal characteristics of each binder used, as determined by standards used to study their burnout kinetics such as thermogravimetric (TGA) and differential scanning calorimetry (DSC) analyses.
- TGA measures weight loss during a temperature ramp, while DSC records the heat flux. By analyzing these data, the optimal temperature and duration for binder burnout can be determined.
- The holding time between heating for burnout can be selected based on the TGA and DSC data, where there is a

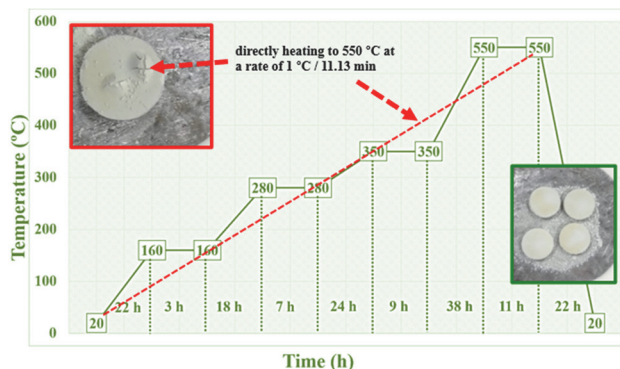


**Fig. 11.** The binder burnout schedule for the sample prepared in Fig. 10(c).

relatively larger weight loss. As seen in Fig. 10, direct heating, without holding time resulted in the cracking of the sample.

- Following the binding process, the resulting samples are subjected to isostatic pressing to increase interparticle contact and remove the vacant spaces created during burned-out binding. Cold isostatic pressing at 200 Mpa is a common technique used for this purpose.

## 5. SINTERING AND DEGREE OF TEXTURE ANALYSIS

- Well-sintered samples can be obtained by careful optimization of the sintering temperature. Well-sintered sample in this case is one in which the matrix grains are nearly consumed by the TGG grain as shown in the schematic Fig. 12(a), which also depends on the sintering time and the amount of the template added. Since we have three variables, such as sintering temperature, sintering time, and BT template amount, first the amount of BT template is fixed to 3 vol% for texturing of 0.4PMN-0.22PZ-0.38PT ceramics, then the sintering temperature varied from 1,000°C, 1,100°C, and 1,200°C at a fixed sintering time of 10 h.
- In Fig. 12(b), the XRD of the random and textured ceramics is shown, where the main XRD peak of, (011) indicated by the arrow, drops as the sintering temperature for the TGG increases, more obvious at 1,200°C, indicating the increase of the degree of texture or increase of the volume fraction of the TGG grain. In the case of a Pb-based system, it is generally recommended that the sintering temperature is not higher than 1,200°C, this is because of the volatile nature of PbO, which can deteriorate the properties of the final textured ceramics. Therefore, the effective approach would be to fix the sintering temperature at 1,200°C for 10 h and increase the BT template amount.
- SEM micrographs in Fig. 13(a) show the cross-section microstructure of the random sample and textured 0.4PMN-0.22PZ-0.38PT ceramics using 3, 5, and 7 vol% of BT template indicating the formation of template grains. From this SEM image, it is difficult to confirm if all matrix grains are consumed or if all grown grains are TGG grains

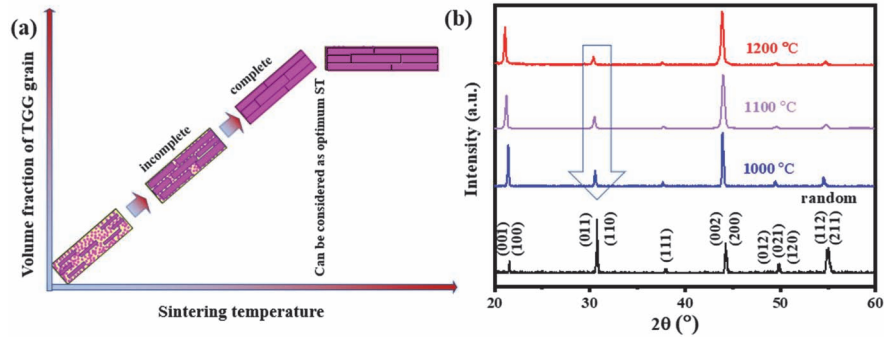


**Fig. 12.** (a) schematic figure on the sintering temperature (ST) versus the volume fraction of the TGG grain and (b) XRD of the random and textured ceramics using 3 vol% of BT template for texturing of 0.4PMN–0.22PZ–0.38PT ceramics at a sintering temperature of 1,000°C, 1,100°C, and 1,200°C at a fixed sintering time of 10 h.

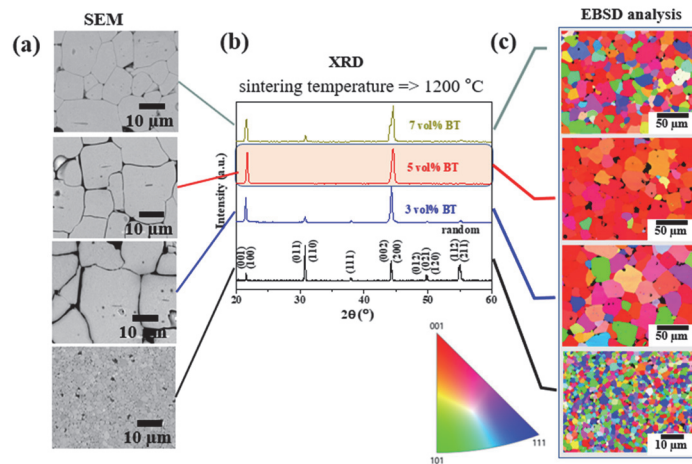


**Fig. 13.** Degree of texture analysis using SEM (a), XRD (b), and EBSD (c) for textured 0.4PMN–0.22PZ–0.38PT ceramics sintered at 1,200°C [the red color in the EBSD map signifies the (001) crystallographic direction].

or oriented in a desired direction.

- XRD data in Fig. 13(b) the peaks other than (00 $l$ ) peak are almost suppressed for the sample containing 5 vol% BT, indicating a higher degree of texture compared to others, confirming that 5 vol% of BT template is optimum.
- The degree of texture can be quantitatively analyzed using multiple random distributions (MRD) analysis (recommended) or Lotgering factor (L.F.) calculated from the XRD profile [10].
- The EBSD analysis in Fig. 13(c) confirms the crystallographic direction with color implementation, where the (001) direction is shown in red, which is more apparent for the sample textured with 5 vol% of BT template.

In conclusion, we discussed challenges associated with TGG processing, such as the size and shape of the templates, their stability in the matrix system, the tape casting process, and the alignment of the templates in the target matrix system, mainly based on our previous published works. We believe that the tutorial can serve as a valuable resource for researchers and engineers seeking to advance their understanding and utilization of the TGG method for producing textured piezoelectric ceramics.

ORCID

Wook Jo

<https://orcid.org/0000-0002-7726-3154>

## ACKNOWLEDGMENTS

This research was supported by the Leading Foreign Research Institute Recruitment Program (No.2017K1A4A3 015437) through the National Research Foundation of Korea (NRF), funded by the Ministry of Science and ICT and UST Young Scientist Research Program 2021 (2021YS28) through the University of Science and Technology of the Republic of Korea.

## REFERENCES

- [1] G. L. Messing, S. Trolier-McKinstry, E. M. Sabolsky, C. Duran, S. Kwon, B. Brahmaroutu, P. Park, H. Yilmaz, P. W. Rehring, K. B. Eitel, E. Suvaci, M. Seabaugh, and K. S. Oh, *Crit. Rev. Solid State Mater. Sci.*, **29**, 45 (2004). [DOI: <https://doi.org/10.1080/10408430490490905>]
- [2] M. M. Seabaugh, G. L. Cheney, K. Hasinska, A. M. Azad, E. M. Sabolsky, S. L. Swartz, and W. J. Dawson, *J. Intell. Mater. Syst. Struct.*, **15**, 209 (2004). [DOI: <https://doi.org/10.1177/1045389X04040131>]
- [3] X. Ding, B. Shen, J. Zhai, Z. Xu, F. Fu, J. Zhang, and X. Yao, *Ferroelectrics*, **401**, 30 (2010). [DOI: <https://doi.org/10.1080/00150191003670366>]
- [4] H. A. Cha, Y. K. Kim, and J. H. Jeon, *J. Eur. Ceram. Soc.*, **37**, 967 (2017). [DOI: <https://doi.org/10.1016/j.jeurceramsoc.2016.10.016>]
- [5] Y. Yan, K. H. Cho, and S. Priya, *J. Am. Ceram. Soc.*, **94**, 1784 (2011). [DOI: <https://doi.org/10.1111/j.1551-2916.2010.04298.x>]
- [6] M. Kim, A. Upadhyay, K. W. Lim, T. T. Zate, and J. H. Jeon, *J. Eur. Ceram. Soc.*, **41**, 7639 (2021). [DOI: <https://doi.org/10.1016/j.jeurceramsoc.2021.08.044>]
- [7] T. T. Zate, M. Kim, and J. H. Jeon, *Sens. Actuators, A*, **335**, 113373 (2022). [DOI: <https://doi.org/10.1016/j.sna.2022.113373>]
- [8] T. Kimura, *Molten Salt Synthesis of Ceramic Powders* (InTech, BoD-Books on Demand, 2011) p. 75-98. [DOI: <https://doi.org/10.5772/20472>]
- [9] A. Buekenhoudt, A. Kovalevsky, J. Luyten, and F. Snijkers, *Comprehensive Membrane Science and Engineering* (2010) p. 217.
- [10] H. L. Yu, N. R. Ko, W. J. Choi, T. T. Zate, and W. Jo, *J. Sens. Sci. Technol.*, **32**, 10 (2023). [DOI: <https://doi.org/10.46670/jsst.2023.32.1.10>]